Journal of Chromatography, 467 (1989) 195–208
Elsevier Science Publishers B.V., Amsterdam — Printed in The Netherlands

CHROM. 21 260

SEPARATION OF NICKEL(II) ALKYLPORPHYRINS BY REVERSED-PHASE HIGH-PERFORMANCE LIQUID CHROMATOGRAPHY

METHODOLOGY AND APPLICATION

CHRISTOPHER J. BOREHAM*
Division of Continental Geology, Bureau of Mineral Resources, Geology and Geophysics, P.O. Box 378, Canberra, 2601 (Australia)
and
CHRISTOPHER J. R. FOOKES
CSIRO, Division of Fuel Technology, Private Mail Bag 7, Menai, NSW 2234 (Australia)
(Received December 29th, 1988)

SUMMARY

Reversed-phase, high-performance liquid chromatography (HPLC) on 4 μm C_{18}-bonded silica has been used to study the elution–structure relationships in a standard set of nickel(II) porphyrins. Nickel(II) etioporphyrins (NiEtio) (C_{27}–C_{32}) were completely separated from later eluting nickel(II)desoxophylloerythroetioporphyrin (NiDPEP) (C_{30}–C_{33}). Structural isomers with a single cycloalkano ring elute before their NiDPEP counterparts unlike species with more than one ring. Within a pseudohomologous series the elution order is t_R β-hydrogen < t_R β-ethyl < t_R β-methyl = t_R β-propyl. Separation of positional isomers is readily achieved. For the NiDPEP series where the site of isomerism is between rings A, B and D, the elution order is t_R ring A < t_R ring B < t_R ring D. Within the NiEtio series t_R ring A ≤ t_R ring C. Nickel(II) alkyl porphyrins of sedimentary origin can be successfully analysed by reversed-phase HPLC. Structural types and individual members can be identified through a combination of retention times, coinjections and absorbance-ratio recording. In doing so the distributions of the structural types can be determined. There is good agreement between this HPLC approach and the assessment of the relative proportions of various structural groups by mass spectrometry.

INTRODUCTION

Petroporphyrins, most likely the fossil biomarkers derived from precursor chlorophylls[1–7] have been used in organic geochemistry as maturation indicators[8–10] and in reconstructing depositional environments[11]. Using their carbon isotopic values in conjunction with isotopic values on coexisting organic matter, various types of secondary processes within sediments which modified the primary photosynthetic organic matter can be determined[12]. These applications usually require a detailed

analysis/isolation of petroporphyrins in order to obtain pure fractions or individual species. High-performance liquid chromatography (HPLC) has been the major analytical technique used in this endeavour.

Metalloporphyrins found in sediments and petroleum are dominated by two metals, nickel(II) (Ni) and vanadium(IV) (as vanadyl, VO)[7]. Usually the metal ion is removed by strong acids and the recovered free-base alkylporphyrins have been analysed by normal-phase high-resolution HPLC on 3-μm or 5-μm silica supports[13,15–17]. In this way, identical HPLC conditions are used to analyse porphyrins chelated to a variety of metals. The separations can utilise polarity as well as basicity differences between the various structural types. However some decomposition of the porphyrin (25% or greater)[18,19] occurs in the strong acid and there is the possibility of preferential loss of different structural types.

Recently, the vanadyl alkylporphyrins have been analysed directly under high-resolution reversed-phase HPLC[18,20] (3-μm C_{18} bonded phase). By comparison, Ni porphyrins are reported to suffer poor resolution and relatively long retention times under similar reversed-phase conditions[16]. Nevertheless, analysis of Ni porphyrins by reversed-phase HPLC has led to the isolation of many compounds with novel structures[2–4,21–24].

The present study reports on the high-resolution reversed-phase HPLC analysis of Ni alkyl porphyrins covering a wide range of structural types. Retention time behaviour is addressed in terms of various substituent characteristics including pseudohomologous series, exocyclic ring size and number, and structural and positional isomerism. Retention time in combination with coinjections and absorbance-ratio recording is used to identify the distribution and relative abundances of structural types in nickel porphyrins of sedimentary origin.

EXPERIMENTAL

Nickel porphyrin standards

Fig. 1 lists the structural types (**1–10**) and members within each structure examined in this study.

Ten authentic samples of free-base porphyrins were generously supplied by Prof. P. Clezy. Nickel(II) was inserted using a published method[22] by adding excess $Ni(acac)_2$ (50:1) to a solution of free-base porphyrin in benzene (1 mg/ml) and refluxing under argon for 5–6 h. In this way, **1b–1i**, **3a** and **7** were obtained.

The remaining Ni porphyrins were isolated from geological samples using thin-layer chromatography and semi-preparative HPLC (see below). The Ni porphyrins with known structures **1a–1i**, **2a–2c**, **2e** and **2f**, **2h**, **3b** and **3c**, **4d**, **5a** and **5b**, **6**, **8a** and **8b**, and **10** were characterised by ^1H NMR (400 MHz) by comparison with literature chemical shifts[2–4,22–26]. Sample **1k** is a complex mixture, while structures of the novel Ni porphyrins **2d**, **2g**, **4a–4c** and **9a** and **9b** are only tentative at present. Chemical shifts, decoupling and limited nuclear Overhauser effect (NOE) experiments firmly established the "lower halves" of the seven structures, but sample limitations have so far prevented the extensive NOE studies required to determine the positions of the substituents in rings A and B.

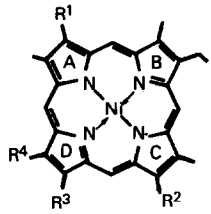

1a: $R^4 = CH_3$, $R^{1-3} = CH_2\ CH_3$ (C_{32})
1b: $R^3 = CH_3$, $R^{1,2,4} = CH_2\ CH_3$ (C_{32})
1c: $R^{1,4} = CH_3$, $R^{2,3} = CH_2\ CH_3$ (C_{31})
1d: $R^{2,4} = CH_3$, $R^{1,3} = CH_2\ CH_3$ (C_{31})
1e: $R^{1,2,4} = CH_3$, $R^3 = CH_2\ CH_3$ (C_{30})
1f: $R^1 = H$, $R^4 = CH_3$, $R^{2,3} = CH_2\ CH_3$ (C_{30})
1g: $R^2 = H$, $R^4 = CH_3$, $R^{1,3} = CH_2\ CH_3$ (C_{30})
1h: $R^1 = H$, $R^{2,4} = CH_3$, $R^3 = CH_2\ CH_3$ (C_{29})
1i: $R^2 = H$, $R^{1,4} = CH_3$, $R^3 = CH_2\ CH_3$ (C_{29})
1j: $R^{1,2} = H$, $R^4 = CH_3$, $R^3 = CH_2\ CH_3$ (C_{28})
1k: Unknown mixture of C_{27} Ni Etio

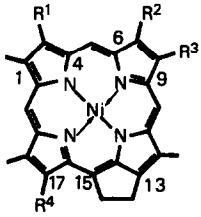

2a: $R^2 = CH_3$, $R^{1,3} = CH_2\ CH_3$, $R^4 = CH_2\ CH_2\ CH_3$ (C_{33})
2b: $R^2 = CH_3$, $R^{1,3,4} = CH_2\ CH_3$ (C_{32})
2c: $R^{1,2} = CH_3$, $R^{3,4} = CH_2\ CH_3$ (C_{31})
2d: $R^{2,3} = CH_3$, $R^{1,4} = CH_2\ CH_3$ (C_{31})
2e: $R^2 = H$, $R^{1,3,4} = CH_2\ CH_3$ (C_{31})
2f: $R^1 = H$, $R^2 = CH_3$, $R^{3,4} = CH_2\ CH_3$ (C_{30})
2g: $R^3 = H$, $R^2 = CH_3$, $R^{1,4} = CH_2\ CH_3$ (C_{30})
or $R^2 = H$, $R^3 = CH_3$, $R^{1,4} = CH_2\ CH_3$ (C_{30})
2h: $R^4 = H$, $R^2 = CH_3$, $R^{1,3} = CH_2\ CH_3$ (C_{30})

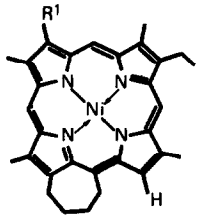

3a: $R^1 = CH_2\ CH_3$ (C_{32})
3b: $R^1 = CH_3$ (C_{31})
3c: $R^1 = H$ (C_{30})

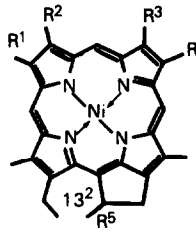

4a: $R^{1,2,3,4}$ 2 x CH_3, 2 x $CH_2\ CH_3$, $R^5 = CH_3$ (C_{33})
4b: $R^{1,2,3,4}$ 3 x CH_3, $CH_2\ CH_3$, $R^5 = CH_3$ (C_{32})
4c: $R^{1,2,3,4}$ H, 2 x CH_3, $CH_2\ CH_3$, $R^5 = CH_3$ (C_{31})
4d: $R^{1,3} = CH_3$, $R^{2,4} = CH_2\ CH_3$, $R^5 = OH$ (C_{32})

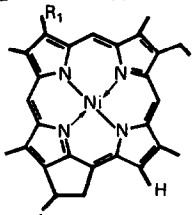

5a: $R^1 = CH_2\ CH_3$ (C_{31})
5b: $R^1 = H$ (C_{29})

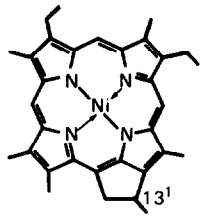

6: (C_{33})

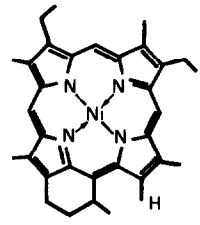

7: (C_{32})

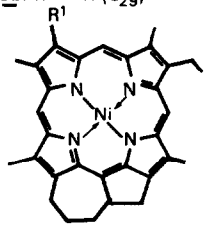

8a: $R^1 = CH_2\ CH_3$ (C_{33})
8b: $R^1 = CH_3$ (C_{32})

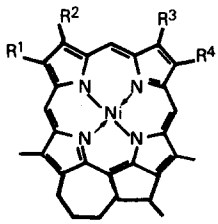

9a: $R^{1,2,3,4}$ 2 x CH_3, 2 x $CH_2\ CH_3$ (C_{34})
9b: $R^{1,2,3,4}$ 3 x CH_3, $CH_2\ CH_3$ (C_{33})

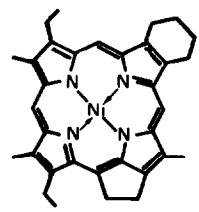

10: (C_{33})

Fig. 1. Structures of standard nickel(II) porphyrins.

Total Ni porphyrins

The total Ni porphyrins from rock extracts and petroleum were separated on silica gel (Merck 40 70–230 mesh) using a progressive solvent gradient from light petroleum (40–60 b.p.) to dichloromethane through a series of three column volume additions of 10, 20, 30, 50, and 70% light petroleum in dichloromethane mixtures; the Ni porphyrins were eluted within the 20–30% additions. This fraction (typically 2–10% in Ni porphyrin) was purified by semi-preparative HPLC and the fraction eluting from the least retained **1j** to the last eluting **10** was collected for detailed analysis by analytical HPLC.

HPLC analyses

Chromatographic separations were performed using Waters equipment: three pumps (two 510 and a 590 series) were programmed through a 680 gradient controller, a U6K injector and a 490 multi-wavelength UV–VIS detector. Synchronous dual-channel detector output [channel 1: ratio recording (the analog output is the ratio of the absorbance at 400 nm to the absorbance at 550 nm), channel 2: absorbance at 400 nm] was interfaced through a 18-bit high-resolution A/D board to the DAPA chromatographic software. Solvents used were pump A: methanol–pyridine (0.2% pyridine); pump B: acetonitrile–pyridine (0.2% pyridine); and pump C: chloroform. Pyridine was freshly distilled before use and all other solvents were HPLC grade and used without further purification. Solvents were kept under a positive helium pressure (Waters eluent stabilization system) during analysis.

Analytical method

Analyses were performed using a precolumn (Guard-Pak μBondapak C_{18}; Waters) and two columns (Nova Pak C_{18} 4 μm, each 150 × 3.9 mm I.D.; Waters) connected in series. Isocratic operation at 1.0 ml/min using methanol–pyridine (0.2% pyridine) gave a back-pressure of 1600 p.s.i. Another column that was tested used Hypersil ODS C_{18} 3 μm. In this case there was no advantage in going to the smaller particle size. Gradient operation employed the program: 0–35 min, 100% A, 1.0 ml/min; linear gradient from 35–65 min, 100% A to 85% A + 15% B, 1.0 ml/min; hold for 5 min.; linear gradient from 70–85 min, 85% A + 15% B to 100% B, 1.0 ml/min to 1.5 ml/min. This was followed by a reconditioning cycle involving a 5 min chloroform wash. Cycle time was two hours.

Semi-preparative method

The semi-preparative separations were performed on a precolumn, two 100 × 8 mm I.D. Nova Pak C_{18} Radial-Pak cartridges and a 300 × 7.8 mm I.D. μBondapak stainless-steel column connected in series. In this case pyridine was not added and the linear solvent program was 0–50 min, 70% A + 30% B to 100% B, 3.0 ml/min and held in acetonitrile mobile phase for a further 25 min. Subsequent washing and reconditioning resulted in a cycle time of 2 h. Back pressures were in the range 900–1600 p.s.i. With this column combination up to 200 μg of total Ni porphyrin could be analysed without overloading.

Mass spectra

Mass spectra were recorded using a VG70E mass spectrometer and VG11/250

data system in the full scan mode (50–650 a.m.u., 2 s scan time). Operating conditions were: electron energy 16 eV, filament current 200 μA, ion source 250°C. Samples (1–2 μg Ni porphyrin) were placed in the direct insertion probe which was temperature programmed. Typically, the probe was rapidly heated from ambient to 150°C and held there until the total ion current decayed to a stable value. The temperature was then programmed to 300°C at 20°C/min. An average spectrum was obtained from the sum of the scans between the first and last detected Ni porphyrins.

RESULTS AND DISCUSSION

Choice of HPLC conditions

Previous reports on the separation of Ni porphyrins under reversed-phase conditions, usually in connection with isolation of single species, have involved the use of a variety of solvents. Most common has been methanol while acetonitrile, ethanol and chloroform have been used in varying concentrations[2–4,21–24].

Preliminary examination in this work using either methanol or acetonitrile resulted in asymmetrical peaks with significant tailing. Considerably shorter elution times occurred with an acetonitrile mobile phase. With the addition of a small percentage (0.2%) of pyridine to the mobile phase, retention times were little affected however a more symmetrical peak shape occurred resulting in an overall two fold increase in column efficiency (32 000 plates/m for **1a**, Fig. 1; this can be compared with 33 000–104 000 plates/m for the HPLC analysis of free-base porphyrins with similar particle size supports[16]). It had been reported that improvements occurred with pyridine addition in the normal-phase HPLC separation of free-base porphyrins[16]. A decrease in porphyrin aggregation and competition for the active sites on the stationary phase had been invoked to explain this improvement.

Separation between and within pseudohomologous series

Elution positions of 35 fully or partially characterised Ni porphyrins were examined and their structures are shown in Fig. 1. In general, the retention times (t_R) for Ni porphyrins with fully alkylated β-substituents which have the five-membered exocyclic alkano ring [nickel(II) desoxophylloerythroetioporphyrin (NiDPEP) series, **2**] are longer than for those without a ring [nickel(II) etioporphyrin (NiEtio) series, **1**]. A similar order was found for free-base porphyrins under normal-phase conditions[17], while the presence of an exocyclic ring had little effect on the elution order for vanadyl porphyrins examined using reversed-phase HPLC[18]. Addition of a methyl substituent to a five-membered exocyclic ring (**4a–4c**, **6**) decreases the retention time while increasing exocyclic alkano ring number increases t_R. The component with two isolated rings (**10**, t_R = 108 min) has a longer retention time than for the species with two fused rings (**8a**, **8b**, **9a** and **9b**, Fig. 2c). This is probably due to a greater interaction between the hydrophobic bonded phase and separated ring systems.

Within a pseudohomologous series, the effect of decreasing the molecular weight through the loss of one methyl group from a β-propyl to a β-ethyl substituent is to decrease the retention time [t_R **2b** < t_R **2a** (not shown, but **2a** coelutes with **2c**, Fig. 2b)]. Presumably the decrease in porphyrin side-chain length results in less interaction with the long aliphatic C_{18} bonded phase. The opposite occurs for a methyl loss involving a β-ethyl to a β-methyl. Here the methyl-substituted member elutes after the higher-

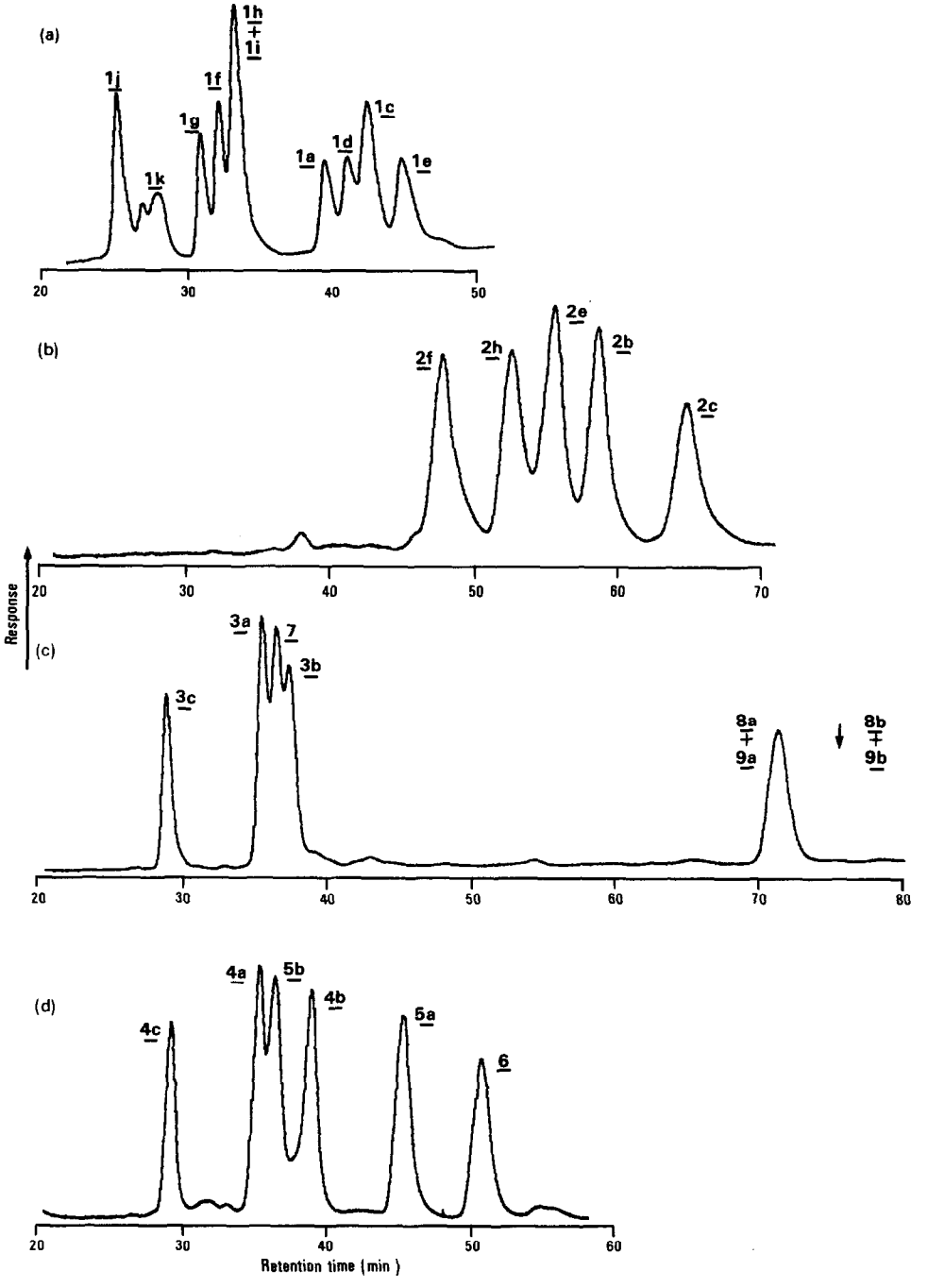

Fig. 2. HPLC traces of synthetic mixtures of standard nickel(II) porphyrins.

carbon-numbered component. Hence t_R **1c** and **1d** > t_R **1a** (Fig. 2a); t_R **2c** and **2d** > t_R **2b** (Fig. 2b); t_R **3b** > t_R **3a** (Fig. 2c); t_R **4b** > t_R **4a** (Fig. 2b); t_R **8b** > t_R **8a** (Fig. 2c); t_R **9b** > t_R **9a** (Fig. 2c). This characteristic elution order is similar to normal-phase HPLC of free-base porphyrins[17]. In the latter the increased retention is governed by the increased polarity of the methyl over the ethyl pseudohomologue. However this cannot be the sole effect which determines retention under reversed-phase HPLC for these Ni porphyrins.

The loss of an additional methyl group gives rise to either a fully alkylated component (2 ethyl groups → 2 methyl groups) or to a β-hydrogen substituent (ethyl → methyl → H). The former results in further retention (t_R **1e** > t_R **1c** and **1d**, Fig. 2a). In the latter, the β-hydrogen member elutes well before the fully alkylated pseudohomologues (again the similarity with free-base porphyrins). Thus within the four pseudohomologous series **1a**, **1c** and **1f**, **2b**, **2c** and **2f**, **3a**–**3c**, and **4a**–**4c**, the member with the β-hydrogen substituent is the least strongly retained followed by the ethyl then the methyl pseudohomologues (Fig. 2a, b, c and d, respectively). For the pseudohomologous series **1f**, **1h** and **1j** the highest-molecular-weight member already has a β-hydrogen while **1j** with two β-hydrogens is the least retained of all the Ni alkylporphyrins studied in this work. An increase in basicity of the alkano-substituted free-base porphyrin (due to their electron-donating effect[27]) was responsible for the greater retention over the β-hydrogen component[17]. With the metalloporphyrins, protonation of the pyrrole nitrogens is unlikely to occur from any residual silanol groups. If this occurred some decomposition of the porphyrin would probably result. Hence the retention of the alkano pseudohomologue may, in part, be the result of an increased electron density in the delocalised porphyrin ring system interacting with the hydrophobic bonded phase.

Addition of a polar hydroxo-group to the five-membered exocyclic ring involves a dramatic decrease in retention time; **4d** elutes at 10 min well before any Ni alkylporphyrin. Here polarity has an overriding influence on retention behaviour.

Structural isomers

For components with the same molecular weight and carbon number, the isomer with a β-hydrogen substituent has a shorter elution time than the fully alkylated counterpart. Thus the two β-hydrogen C_{30} NiEtio (**1f** and **1g**) elute well before the fully alkylated isomer, **1e**. The same elution order occurs for the C_{30} NiDPEP isomers (t_R **2e** < t_R **2c** and **2d**). The two C_{32} components with a β-hydrogen, the methyl-substituted six-membered ring (**7**) and the seven-membered ring (**3a**), also elute before the fully alkylated five-membered ring C_{32} NiDPEP (**2b**). Also **3a** has a slightly shorter t_R than **7**. Of interest are the relative t_R values of the novel porphyrins with methyl-substituted five-membered rings (**4**, **5** and **6**) and their NiDPEP counterparts (**2**). For the isomers with β-hydrogens, the elution order is t_R **4b** < t_R **5a** < t_R **2e**, even though the presence of a β-methyl group in **4b** compared with a β-ethyl substituent in the other two would help in its retention (see previous heading). The fully alkylated isomers with the methyl-substituted five-membered ring C_{32} (**4b**) and C_{33} (**4a** and **6**), elute well before their respective C_{32}NiDPEP (**2b**) and C_{33}NiDPEP (**2a**) isomers.

Positional isomers

In most cases, positional isomers can be resolved by reversed-phase HPLC. For

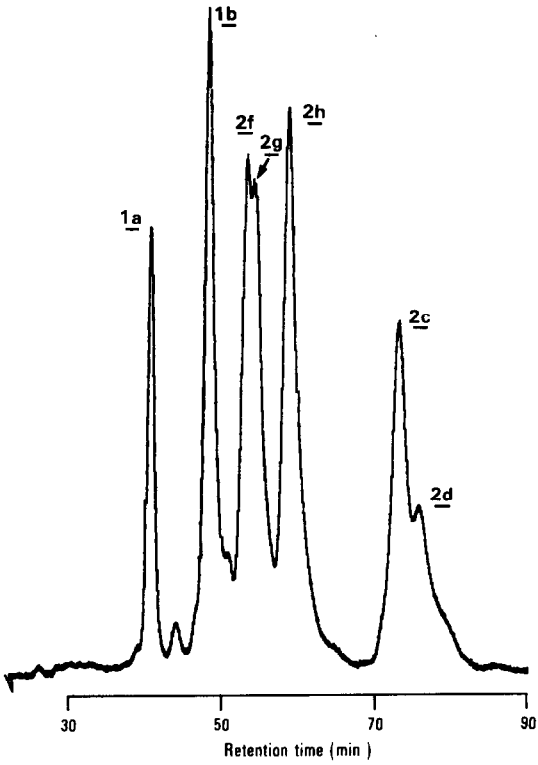

Fig. 3. HPLC trace of various positional isomers of standard nickel(II) porphyrins.

example, there is complete separation of Ni etioporphyrin III (**1a**) and Ni etioporphyrin I (**1b**) (Fig. 3). Other positional isomers which show baseline resolution are the ring A-β-hydrogen NiC_{30}DPEP (**2f**) from the ring D-β-hydrogen NiC_{30}DPEP (**2h**) (Figs. 2b and 3) and the 13(2)-methyl-substituted (13,15-ethano-) five-membered ring C_{31} species (**4c**) from the 15(2)-methyl-substituted (15,17-ethano-) five-membered ring C_{31} isomer (**5a**) (Fig. 2d). Partial separation occurs between: ring A-methyl and ring C-methyl NiC_{31}Etio (**1c** and **1d**, Fig. 1a) and likewise their respective β-hydrogen C_{30} pseudohomologues (**1f** and **1g**, Fig. 1a); ring A-methyl and ring B-methyl NiC_{31}DPEP (**2c** and **2d**, Fig. 3); ring A-β-hydrogen and ring B-β-hydrogen NiC_{30}DPEP (**2f** and **2g**, Fig. 3). The two NiC_{29}Etio positional isomers (**1h** and **1i**, Fig. 1a) coelute.

These preliminary results suggest that for Ni porphyrins of the DPEP type (**2**), the elution order for positional isomers is t_R ring A $<$ t_R ring B $<$ t_R ring D while for the NiEtio porphyrins (**1**) the order is t_R ring A $\leqslant$ t_R ring C. It is interesting to look at the two C_{33} isomers which have methyl-substituted five-membered rings. For isomer **4a** the methyl group is attached to the 13(2) carbon while for **6** it is bound to the 13(1) carbon. The shorter t_R for **4a** probably results from less effective interaction with the bonded stationary phase due to steric hindrance between the methyl group and the adjacent ring D ethyl group.

Application

Fig. 4a shows the HPLC trace under isocratic conditions of a synthetic mixture obtained on combining the mixtures in Fig. 2a–d. Severe overlap is evident in parts of the chromatogram making assignments difficult. Using the gradient program, elution times have been considerably reduced (*e.g.* **10** elutes in 80 min *cf.* 108 min previously) while elution orders remain the same (Fig. 4c *cf.* Fig. 4a).

The values for the ratio of the absorbance at 400 nm to the absorbance at 550 nm is given in Table I for all the standard Ni porphyrins. It covers a wide range from 1.4 for **1** to 9.5 for Ni butano-porphyrin **3** although it is slightly solvent dependent. For a pure single compound the absorbance-ratio plot should be a constant value over the elution profile of the peak. In Fig. 4b the ratio plot overlies the absorbance trace (Fig. 4c) and maintains a uniform value over the bulk of the peak. The slight variation in the ratio

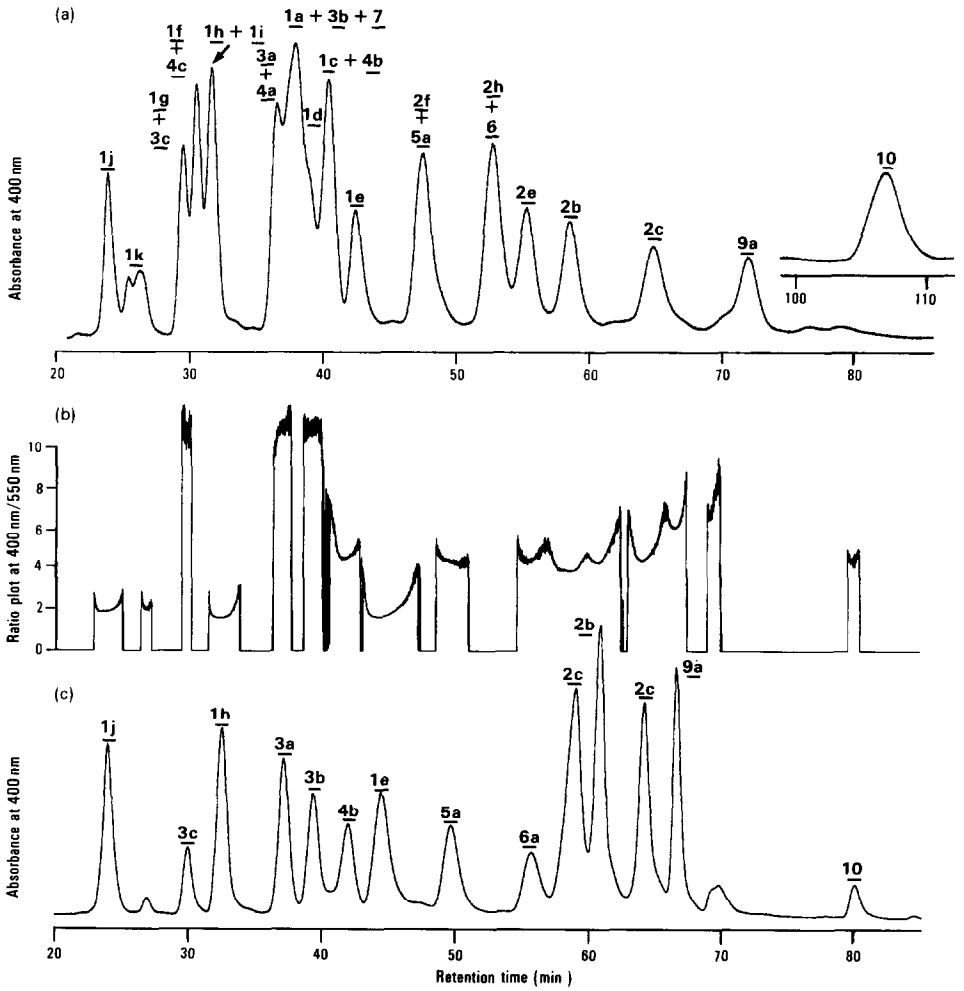

Fig. 4. HPLC traces of standard nickel(II) porphyrin mixtures. (a) Isocratic (methanol–0.2% pyridine), (b) ratio plot corresponding to absorbance plot in (c), (c) gradient program (see Experimental).

value over the total peak might be due to some impurities. A more likely explanation is that changes in porphyrin aggregation over the peak profile cause slight perturbations in the absorbance spectrum, hence ratio trace.

This dual detection approach (absorbance and absorbance-ratio monitoring) is therefore invaluable in deconvoluting coeluting or closely eluting components under the HPLC conditions used here. In a total Ni porphyrin fraction of sedimentary origin, the diverse array of structural types usually means coelutions are inevitable. Fig. 5 depicts the absorbance and ratio traces of non-polar Ni alkylporphyrins from two immature shales —the marine Julia Creek oil shale (Fig. 5a, 1401) and the lacustrine Messel oil shale (Fig. 5b, 4208). Ni porphyrins from both sediments have been extensively studied and numerous single species isolated[2–4,28,29].

The two major peaks eluting in the "Etio region" of the chromatogram for the Julia Creek sample were identified as the Ni butano porphyrins **3a** and **3b** on the basis of their retention times and high absorbance-ratio values. The slightly lower ratio observed here (Fig. 5a) than for the pure butano standards (Fig. 4b) results from minor contributions from coeluting porphyrins which have a much lower absorbance-ratio (Fig. 4a and Table I). The major component in the Messel sample was identified as the methyl-substituted (15,17 ethano-) five-membered ring porphyrin, **5a**. Although the β-hydrogen C_{30}NiDPEP (**2f**) coelutes with **5a** (Fig. 4a), the latter complex has a slightly higher absorbance-ratio (Table I). This species, first isolated as the major component in the Messel shale, is thought to be derived from chlorophyll c[24].

In order to establish relative abundances of the various structural types, the relative values for the extinction coefficients must be known at the monitoring wavelength (*i.e.* 400 nm). The Soret maxima (λ_{max}) for the standard Ni porphyrins ranges from 392 nm (**1**) to 400 nm (**3**) and is uniform within structural types. Absolute extinction coefficients (ε_{max}) have been determined for all the structural types at λ_{max} and all lie within the range 180 000–220 000 (ref. 30). The close similarity in extinction coefficients is further confirmed as follows; relative concentrations of standard mixtures of **1d**, **2b**, **3a** and **3b** were estimated from the visible spectrum using the same ε_{max} and agree to within 10% those obtained from molecular ion abundances. Hence the normalising factor for the relevant structural type relative to **3** is equal to (ε_{max} structural type/ε_{max} for **3**) × (absorbance at λ_{max}/absorbance at λ_{400}). Thus the

TABLE I

VALUE FOR THE RATIO OF ABSORBANCE AT 400 nm TO ABSORBANCE AT 550 nm (IN METHANOL–0.2% PYRIDINE)

Ni por.	*Ratio*	*Ni por.*	*Ratio*	*Ni por.*	*Ratio*	*Ni por.*	*Ratio*
1a	1.48	**1j**	1.79	**2h**	3.60	**5b**	3.87
1b	1.41	**1k**	1.76	**3a**	9.45	**6**	3.47
1c	1.42	**2a**	3.35	**3b**	9.45	**7**	4.63
1d	1.43	**2b**	3.35	**3c**	9.20	**8a**	4.60
1e	1.43	**2c**	3.28	**4a**	3.80	**8b**	4.50
1f	1.54	**2d**	3.25	**4b**	3.73	**9a**	5.00
1q	1.55	**2e**	3.30	**4c**	3.45	**9b**	4.93
1h	1.50	**2f**	3.33	**4d**	2.10	**10**	3.20
1i	1.46	**2g**	3.35	**5a**	3.73		

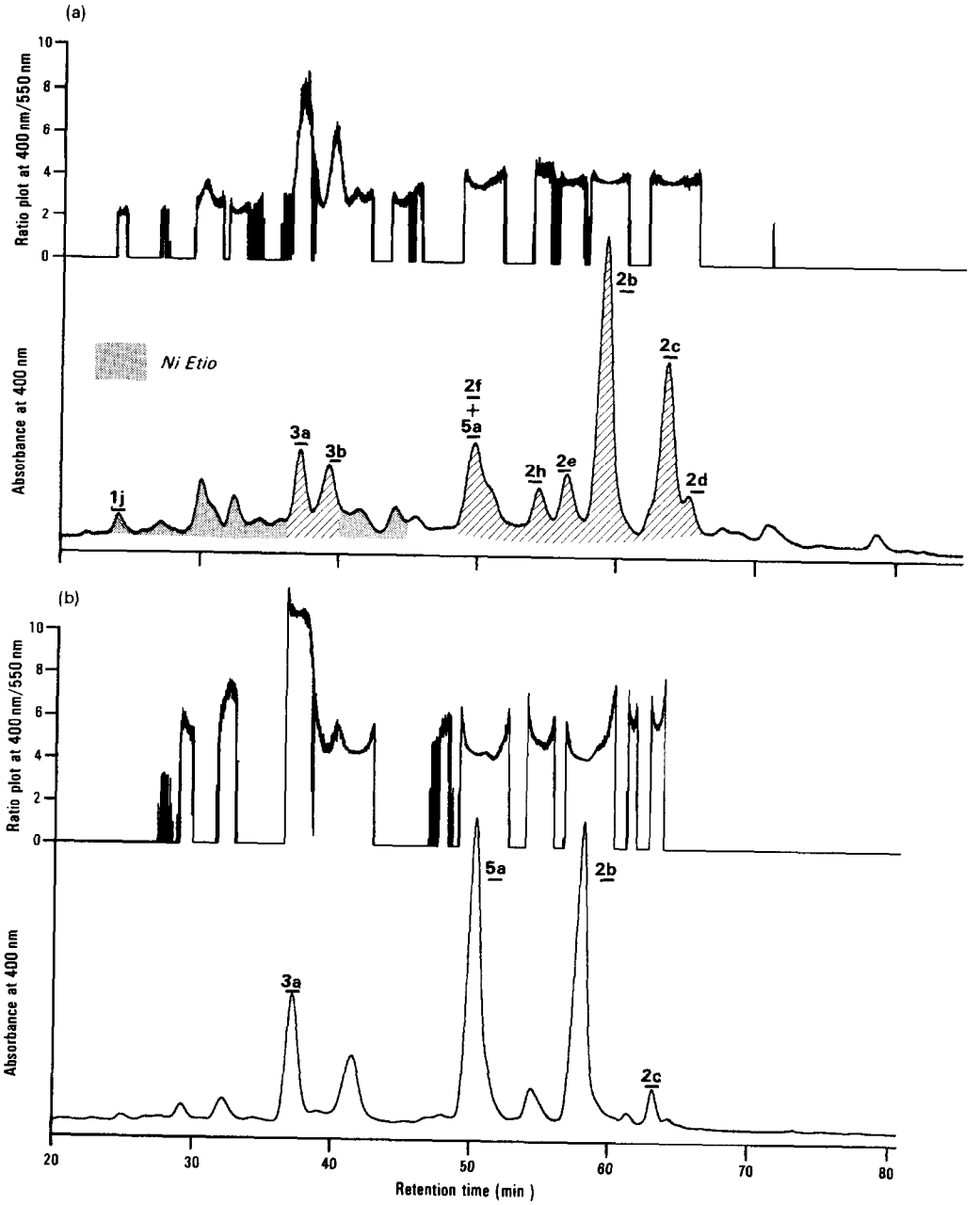

Fig. 5. HPLC traces of total nickel(II) porphyrins from (a) Julia Creek oil shale (1401), (b) Messel oil shale (4208).

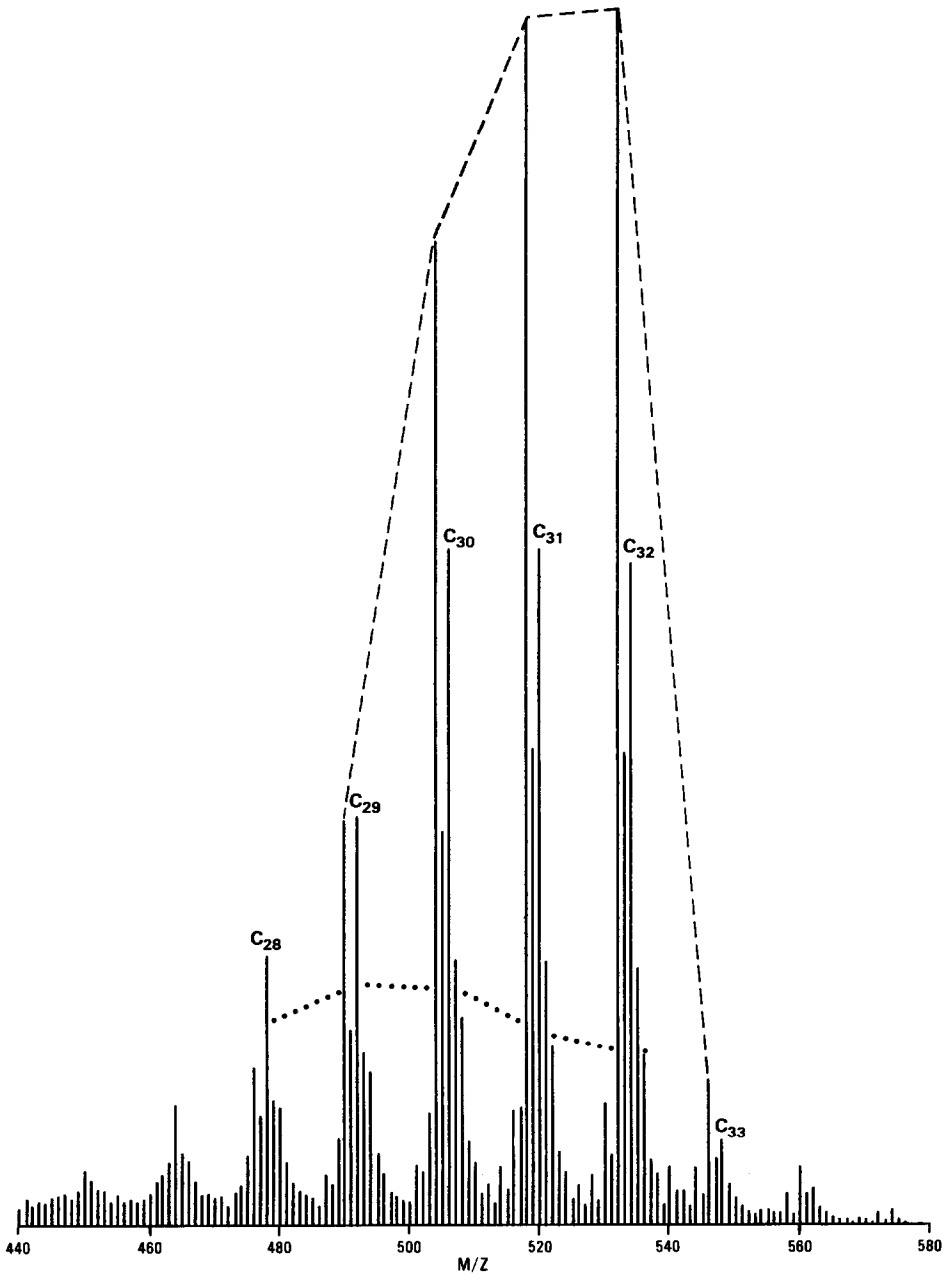

Fig. 6. Low voltage (16 eV) mass spectrum of the nickel(II) porphyrins from Julia Creek oil shale. (— — —) Monoexocyclic ring ^{58}Ni porphyrin; (.....) ^{58}NiEtio.

integrated areas are multiplied by this normalising factor and for **1**, **2**, **3**, **4**, **5**, **6**, **7**, **8**, **9** and **10** this value is equal to 1.91, 1.41, 1.0, 1.25, 1.29, 1.33, 1.09, 1.26, 1.21 and 1.30, respectively.

As an example, this approach was applied to the analysis of the Ni porphyrins in the Julia Creek sample. The integrated areas of the C_{28}–C_{32} NiEtio porphyrins (Fig. 5a) were summed and normalised as were those for the butano and DPEP series (other single exocyclic structures were very minor in comparison). The percentage of the NiEtio porphyrins was 20.6%. A complementary method which can give similar information is mass spectrometry. Here structural types can only be differentiated on the basis of the number of exocyclic rings because these give rise to molecular ions separated in steps of two daltons. After correction for the isotopic contribution from ^{13}C, ^{2}H and $^{60}Ni^{31}$ (molecular ion of a ^{60}Ni porphyrin with a single exocyclic ring is the same nominal mass number as the idential carbon numbered ^{58}NiEtio porphyrin), the percentage of C_{28}–C_{32} NiEtio porphyrins to C_{29}–C_{33} Ni porphyrins with one exocyclic ring was 19.5% (Fig. 6). This close agreement between the two unrelated techniques clearly demonstrates that reversed-phase HPLC of Ni porphyrins is a viable technique for determining the relative distribution of various structural types.

CONCLUSIONS

(1) Reversed-phase HPLC on 4-μm C_{18} bonded silica can be successfully used to separate nickel(II) alkylporphyrins covering a variety of structural types. Although the efficiency (plates/m) is less than that obtained for free-base porphyrins using similar particle-size stationary phases, good resolution is obtained in mostly acceptable elution times.

(2) The NiEtio porphyrins (C_{27}–C_{32}) are completely separated from the NiDPEP series (C_{30}–C_{33}).

(3) Within a pseudohomologous series, the elution order is t_R β-hydrogen $< t_R$ β-ethyl $< t_R$ β-methyl. For the cycloalkanoporphyrins with one isolated ring, the structural isomers of the DPEP type have the longest elution times. The addition of a second alkano ring system leads to further retention in which two isolated rings are retained longer than for two fused rings. Separation of positional isomers can be achieved and for the NiDPEP isomers t_R ring A $< t_R$ ring B $< t_R$ ring D, while for the NiEtio isomers t_R ring A $\leqslant t_R$ ring C.

(4) The combination of retention time, coinjection of authentic standards and absorbance-ratio recording is a powerful technique in the identification of Ni porphyrins with different structural types and individual members within each type.

(5) Reversed-phase HPLC of Ni porphyrins can be used to obtain reliable information on the relative abundances of various structural types without the need for demetallation.

ACKNOWLEDGEMENTS

We thank Mr. Algis Juodvalkis for his technical assistance and Prof. Peter Clezy for synthetic free-base porphyrins. C.J.B. publishes with the permission of the Director, Bureau of Mineral Resources, Geology and Geophysics.

REFERENCES

1 J. M. E. Quirke, G. Eglinton and J. R. Maxwell, *J. Am. Chem. Soc.*, 101 (1978) 7693.
2 C. J. R. Fookes, *J. Chem. Soc., Chem. Commun.*, (1983) 1472.
3 C. J. R. Fookes, *J. Chem. Soc., Chem. Commun.*, (1983) 1474.
4 C. J. R. Fookes, *J. Chem. Soc., Chem. Commun.*, (1985) 706.
5 A. Ekstrom, C. J. R. Fookes, T. Hambley, H. J. Loeh, S. A. Miller and J. C. Taylor, *Nature (London)*, 206 (1983) 173.
6 M. I. Chicarelli, S. Kaur and J. R. Maxwell, in R. H. Filby and J. F. Branthaver (Editors), *Metal Complexes in Fossil Fuels (ACS Symp Series* 344), Washington, DC, 1987, pp. 41–67.
7 E. W. Baker and J. W. Louda, in R. B. Johns (Editor), *Biological Markers in the Sedimentary Record*, Elsevier, New York, 1986, pp. 124–225.
8 A. J. G. Barwise and P. J. D. Park, in M. Bjorøy (Editor), *Advances in Organic Geochemistry, 1981*, Wiley, London, 1983, pp. 668–674.
9 J. Shi, A. S. Mackenzie, R. Alexander, G. Eglinton, A. P. Gower, G. A. Wolff and J. R. Maxwell, *Chem. Geol.*, 35 (1982) 1.
10 A. J. G. Barwise, in R. H. Filby and J. F. Branthaver (Editors), *Metal Complexes in Fossil Fuels (ACS Symp. Series* 344), Washington, DC, 1987, pp. 100–109.
11 J. Moldowan, P. Sundararaman and M. Schoell, *Org. Geochem.*, 10 (1986) 915.
12 R. Takigiku, *Ph.D. Thesis*, Indiana University, Bloomington, IN, 1987.
13 S. K. Hajibrahim, P. J. C. Tibbetts, C. D. Watts, J. R. Watts, G. Eglinton, H. Colin and G. Guiochon, *Anal. Chem.*, 50 (1978) 549.
14 J. M. E. Quirke, in R. H. Filby and J. F. Branthaver (Editors), *Metal Complexes in Fossil Fuels (ACS Symp. Series* 344), Washington, DC, 1987, pp. 308–337 and references therein.
15 A. S. MacKenzie, J. M. E. Quirke and J. R. Maxwell, in A. G. Douglas and J. R. Maxwell (Editors), *Advances in Organic Geochemistry, 1979*, Pergamon Press, Oxford, 1980, pp. 239–248.
16 A. J. G. Barwise, R. P. Evershed, G. A. Wolff, G. Eglinton and J. R. Maxwell, *J. Chromatogr.*, 368 (1986) 1.
17 M. I. Chicarelli, G. A. Wolff and J. R. Maxwell, *J. Chromatogr.*, 368 (1986) 11.
18 P. Sundararaman, *Anal. Chem.*, 57 (1985) 2204.
19 C. J. Boreham, unpublished results.
20 P. Sundararaman, W. R. Biggs, J. C. Reynolds and J. C. Petzer, *Geochim. Cosmochim. Acta.*, 52 (1988) 2337.
21 R. Ocampo, H. J. Callot and P. Albrecht, *J. Chem. Soc., Chem. Commun.*, (1985) 198.
22 J. Verne-Mismer, R. Ocampo, H. J. Callot and P. Albrecht, *Tetrahedron Lett.*, 27 (1986) 5257.
23 J. Verne-Mismer, R. Ocampo, H. J. Callot and P. Albrecht, *J. Chem. Soc., Chem. Commun.*, (1987) 1581.
24 R. Ocampo, H. J. Callot and P. Albrecht, *Tetrahedron*, 40 (1984) 4033.
25 J. Krane, T. Skjetne, N. Telnaes, M. Bjorøy, L. Schol and H. Solli, *Org. Geochem.*, 6 (1984) 193.
26 P. S. Clezy, C. J. R. Fookes and J. K. Prasher, *Aust. J. Chem.*, submitted for publication.
27 P. Hambright, in K. Smith (Editor), *Porphyrins and Metalloporphyrins*, Elsevier, Amsterdam, 1976, pp. 236–278.
28 C. J. Boreham and T. G. Powell, *Org. Geochem.*, 11 (1987) 433.
29 R. Ocampo, H. J. Callot and P. Albrecht, in R. H. Filby and J. F. Branthaver (Editors), *Metal Complexes in Fossil Fuels (ACS Symp. Series* 344), Washington, DC, 1987, pp. 68–73.
30 B. N. Popp, J. M. Hayes and C. J. Boreham, *Org. Geochem.*, submitted for publication.
31 J. W. Louda and E. W. Baker, in R. S. Yeats, B. U. Hag *et al.*, *Initial Reports of the Deep Sea Drilling Project, Vol. LXIII*, U.S. Government Printing Office, Washington, DC, 1981, pp. 785–817.